HHS Public Access

Author manuscript

J Immunol. Author manuscript; available in PMC 2018 January 15.

Published in final edited form as:

J Immunol. 2017 January 15; 198(2): 757–766. doi:10.4049/jimmunol.1600759.

Kinetics of myeloid derived suppressor cell frequency and function during SIV infection, combination antiretroviral therapy and treatment interruption[1]

Sandra E Dross[*,†], **Paul V Munson**[‡,§], **Se Eun Kim**[†], **Debra L Bratt**[§], **Hillary C Tunggal**[‡,§], **Ana L Gervassi**[†], **Deborah H Fuller**[‡,§], and **Helen Horton**[*,¶]

[*] Department of Global Health, University of Washington, Seattle, WA

[†] Center for Infectious Disease Research, Seattle, WA

[‡] Department of Microbiology, University of Washington, Seattle, WA

[§] Washington National Primate Research Center, Seattle, WA

[¶] Immune Modulation Research, Janssen Infectious Diseases & Vaccines BVBA, Beerse, Belgium.

Abstract

During chronic lentiviral infection, poor clinical outcomes correlate both with systemic inflammation and poor proliferative ability of HIV-specific T cells, however the connection between the two is not clear. MDSC[2], suppressive myeloid cells that expand during states of elevated circulating inflammatory cytokines, may link the systemic inflammation and poor T cell function characteristic of lentiviral infections. While MDSC are partially characterized in HIV and SIV infection, questions remain regarding their persistence, activity and clinical significance. We monitored MDSC frequency and function in SIV infected rhesus macaques. Low MDSC frequency was observed prior to SIV infection. Post-SIV infection, MDSC were elevated in acute infection and persisted during 7 months of cART[3]. After cART interruption, we observed MDSC expansion of surprising magnitude, the majority being gMDSC[4]. At all stages of infection, gMDSC suppressed CD4+ and CD8+ T cell proliferation in response to polyclonal or SIV-specific stimulation. In addition, MDSC frequency correlated significantly with circulating inflammatory cytokines. Acute and post-cART levels of viremia were similar, however, the levels of inflammatory cytokines and MDSC were more pronounced post-cART. Expanded MDSC during SIV infection, especially during the post-cART inflammatory cytokine surge, likely limit cellular responses to infection. As many HIV curative strategies require cART interruption to determine efficacy, our work suggests treatment interruption-induced MDSC may especially undermine

[1]Research reported in this publication was supported by NIAID, NCI, NIMH, NIDA, NICHD, NHLBI, NIA, NIGMS, NIDDK of the National Institutes of Health under award number AI027757, the National Institutes of Health Grant R01 AI104679-01, and Janssen Infectious Diseases &Vaccines BVBA, Beerse, Belgium.

[2]MDSC, myeloid derived suppressor cells

[3]cART, combination antiretroviral drug therapy

[4]gMDSC, granulocytic myeloid derived suppressor cells

Corresponding author: Sandra Dross, Center for Infectious Disease Research, 307 Westlake Ave N, Seattle WA 98105, Phone: (206) 256-7258, Fax: (206) 256-7229, Sandra.dross@cidresearch.org.

effectiveness of such strategies. MDSC depletion may enhance T cell responses to lentiviral infection and effectiveness of curative approaches.

Introduction

MDSC are a heterogeneous group of immunosuppressive cells of myeloid origin (reviewed in (1)). MDSC were originally described, and have canonically been characterized, in mouse tumor models and cancer patients, where they inhibit anti-tumor responses and correlate with poor clinical outcomes and tumor burden (2, 3). When MDSC are ablated, both natural and vaccine-induced anti-cancer immune responses are efficacious at delaying or controlling tumor growth (4-6). MDSC suppress T cell responses by four classes of mechanisms: amino acid restriction, modulation of trafficking and viability, generation of reactive oxygen and nitrogen species, and T regulatory cell induction (reviewed in (1)).

While cells of similar phenotype and function were described as myeloid-suppressor cells (MSC) starting in 2000, and null cells, veto cells, or natural suppressor (NS) cells in the mid-1900s, the identifier MDSC is relatively new as it was first mentioned in the literature in 2005 (reviewed in (2)). MDSC are characterized by the presence of myeloid markers (for humans, marker CD11b or CD33) and absence of lineage commitment markers (lack of HLA-DR, or Lin-). Recently, many groups have further characterized gMDSC and mMDSC[5] subsets; MDSC of granulocytic (granulocyte marker CD15+ or CD66+) or monocytic (monocyte marker CD14+) nature. The granulocytic subset of MDSC consists of low-density granulocytes at varying stages of maturation (7-9).

During pathogenic lentiviral infections including HIV and SIV, cellular and humoral immune responses are insufficient to clear acute infection, leading to persistent infection and disease progression for most individuals. In these individuals, despite initial effective cellular responses critical for viral control, T cells lose functional capacity leading to disease progression (10). A small subset of individuals called HIV controllers or long-term nonprogressors maintain T cell polyfunctionality and proliferative ability (11), retaining the ability to control viral replication and disease progression in the absence of antiretroviral therapy. Of T cell functions, loss of proliferative ability in response to HIV-stimulation is the strongest independent predictor of progression vs. control (12). Systemic inflammation is a hallmark of chronic pathogenic lentiviral infections and contributes greatly to the immune dysfunction observed. In lentiviral infection chronic systemic inflammation is induced via viral replication and microbial translocation and is dampened but persists during virologic suppression (13, 14). Indeed, immune activation correlates more strongly with poor prognosis than viral load or coreceptor use alone (15).

The causes of T cell dysfunction in progressive infection and the link between cellular dysfunction and immune activation dependent disease outcomes are not yet completely understood. Inflammation during acute infection serves to drive and tune the innate and adaptive immune responses but persists as these responses are insufficient to resolve viral

[5]mMDSC, monocytic myeloid derived suppressor cells

infection. Additionally, microbial translocation due to loss of gut barrier integrity continues to drive inflammation even in the absence of viral replication. We suspect MDSC are expanded and activated due to inflammation resulting from viral replication and microbial translocation and that, subsequently, these MDSC contribute to immune dysfunction by suppressing the proliferative capacity of virus-specific T cells.

Previous studies showed increased frequencies of gMDSC and mMDSC in HIV+ vs. HIV− individuals that correlated with high viral loads, low CD4 counts, increasing T cell activation, and advanced disease stage (16-18). In SIV infection, studies have shown a CD8+ T cell suppressive mMDSC-like population of monocytes in a pigtailed macaque (*Macaca nemestrina*) SIV infection model that decrease in frequency during cART treatment (19). MDSC have been studied in the context of prophylactic SIV vaccine and were significantly elevated in the vaccination but not in the control group, which displayed better virologic control and no less protection from infection compared to the vaccinated group. This suggests MDSC were elicited by the vaccine in this study, hampering immune control of SIV. These MDSC suppressed CD8+ T cell proliferative responses to SIV in a dose-dependent manner and correlated with higher set-point viral load (20).

As these studies were either cross-sectional or had a limited sampling timeline, the pervasiveness, activity and clinical consequences of MDSC over the course of infection are unknown. In addition, it is not clear if elevations in MDSC frequency predate the acquisition of virus. Also uncertain is the impact of cART-treatment interruption on MDSC populations. We followed 7 animals over the course of SIV infection, treatment with cART and cART-interruption to examine the kinetics of MDSC frequency, their function in chronic retroviral infections and their relationship to inflammatory cytokine responses. Here we show gMDSC are elevated and suppressive in acute and cART-treated chronic lentiviral infection. At cART-interruption we show a remarkable increase in gMDSC that correlates significantly with a secondary and enhanced inflammatory cytokine elevation.

Materials and methods

Specimen collection

Rhesus macaque (*Macaca mulatta)* blood and tissue were obtained from the Washington National Primate Research Center. A total of 19 adult male Indian-origin rhesus macaques were used in this study. All animal protocols were reviewed and approved by the Institutional Animal Care and Use Committee at the University of Washington and were in compliance with the U.S. Department of Health and Human Services Guide for the Care and Use of Laboratory Animals. Animals were infected IV with SIV/DeltaB670. Blood draws in the first pilot study were obtained 12 weeks post-SIV infection with no cART (Fig. 1A). Longitudinal study blood draws were obtained over the course of SIV infection including study weeks −4, −3, 2, 3, 10, 14, 18, 36, 37, 40, 46, 56, 68 and 80. Animals were SIV infected at study week 0 and put on cART at study week 6. The cART regimen consisted of daily subcutaneous Viread (PMPA, 20 mg/kg), Emtriva (FTC, 30 mg/kg until viral suppression then 20 mg/kg), and twice-daily oral Isentress (Raltegravir, 200mg/kg first 30 days treatment then 165mg/kg). Animals followed for MDSC kinetics were control animals for a therapeutic vaccine study and received mock vaccine consisting of an empty plasmid

vector +/− plasmid-encoded LT[6] mucosal adjuvant at study weeks 18, 22, 26 and 30. cART-cessation occurred at week 37 and animals were followed every 10 weeks until AIDS-defining illness or necropsy at week 80 when blood and tissues were obtained (Fig. 1B). Blood was drawn into 10ml sodium heparin tubes, transferred at room temperature and processed immediately. All experiments were performed with freshly isolated PBMC. Tissue was excised at necropsy, placed in 25ml RPMI, transferred to CIDR on wet ice and processed immediately.

Blood processing

Plasma was isolated for later cytokine analysis via centrifugation, and PBMC were obtained by density separation using Ficoll-Paque PREMIUM (GE Healthcare). PBMC were rinsed with PBS and resuspended in EasySep™ Buffer (Stemcell Technologies) for staining and MDSC isolation.

Staining

Freshly isolated PBMC were stained for MDSC frequency using CD3 clone SP34-2 Pacific Blue (Becton Dickinson), CD11b clone ICRF44 PeCy7 (Miltenyi Biotec), CD14 clone m5e2 APC (Becton Dickinson), CD16 clone 3g8 PECy5 (Becton Dickinson), CD66 clone TET2 PE (Miltenyi Biotec), HLA-DR clone L243 APC-Cy7 (Fisher Scientific). Gating strategy for gMDSC was all PBMC, singlets, CD3−, HLA-DR−, CD11b+, and for gMDSC, CD66+, $SSC^{mid\text{-}high}$ while for mMDSC, CD66− and CD14+. Gating was determined by FMO and compensation control values. MDSC frequency was calculated based on % mMDSC or gMDSC of singlet PBMC.

MDSC isolation and PBMC co-cultures

CD66+ MDSC were separated from PBMC as per kit instructions using magnetic bead isolation (EasySep™) of PE-conjugated anti-CD66 (Miltenyi Biotec). CD66− PBMC were cultured at 37°C, 5% CO_2, overnight either alone or with CD66+ MDSC added back at a 1:1 ratio in custom arginine-low media: SILAC media (Sigma Aldrich) plus filter-sterilized L-arginine monohydrochloride (0.115mM, Sigma Aldrich) and filter-sterilized L-lysine hydrochloride (0.2186mM, Sigma Aldrich), 15% human serum (Sigma Aldrich), Penicillin-Streptomycin-Glutamine (0.5mg/ml, Thermo Fisher). Cells were stimulated with 1ug/ml 15mer SIVmac239 Gag peptide pool (NIH AIDS Reagent Program) or 0.4ug/ml superantigen SEB[7] from *Staphylococcus aureus* (Sigma Aldrich) for 4 days. Duplicate control un-stimulated wells for each cell mixture (PBMC alone, PBMC with CD66+MDSC) were included for background proliferation subtraction. Proliferation was measured by ICS on day 4 post-stimulation using CD8 clone SK1 PECy7 (Biolegend), Ki67 clone B56 Alexa Flour 488 (Becton Dickinson), CD3 clone SP34-2 APC (Becton Dickinson). CD66+ MDSC-mediated suppression was measured by comparing the proliferation stimulated in the absence of CD66+ cells with the proliferation stimulated in the presence of CD66+ cells. Replicates were included for all PBMC wells, and PBMC + MDSC when MDSC yield allowed, and averaged.

[6]LT, heat labile *E. coli* enterotoxin
[7]SEB, Staphylococcal enterotoxin B

TNF cultures

Whole PBMC were incubated 2 days with 10ng/ml TNF in low-arginine media then measured for gMDSC by CD66 clone TET2 PE (Miltenyi Biotec), HLA-DR clone L243 APC-Cy7 (Fisher Scientific), LIVE/DEAD Fixable Violet (Life Technologies), and proliferation by ICS for Ki67 clone B56 Alexa Flour 488 (Becton Dickinson).

IFNγ ELISpot

IFNγ release upon SEB stimulation of PBMC with and without MDSC (1:1 or 1:0 ratio) was determined as previously published (21) with modifications: experiments were performed in triplicate in low-arginine media with rhesus IFNγ capture mAb MD-1 (UCytech), biotinylated anti-monkey IFNγ Ab (U-Cytech) and an 18 hour incubation time for IFNγ release.

Tissue processing at necropsy

Single-cell suspensions were made of ileum, spleen, and axillary, ileocecal, iliac, inguinal, mesenteric, cervical and retropharyngeal lymph nodes in 25ml RPMI, passed through a 100um filter and density separated with Ficoll-Paque PREMIUM (GE Healthcare). Buffy coats for each tissue were rinsed with PBS, resuspended in EasySep™ Buffer (Stemcell Technologies) and stained for MDSC.

Plasma Cytokine Levels

Plasma was frozen at −80°C immediately during blood processing, then batch tested as per kit instructions using the Monkey Cytokine Magnetic 29-Plex Panel (ThermoFisher) for the following cytokines, chemokines and growth factors: GM-CSF, TNF, IL-1β, IL-4, IL-6, MIG[8], VEGF[9], HGF[10], EGF[11], IL-8, IL-17, MIP-1α, IL-12, IL-10, FGF-Basic[12], IFN-γ, G-CSF, MCP-1[13], IL-15, IP-10[14], MIP-1β, Eotaxin, RANTES, IL-1RA[15], I-TAC[16], MDC[17], IL-5, IL-2, and MIF[18].

sCD14 ELISA

Plasma was isolated, frozen and batch tested for sCD14 at study weeks 0, 2, 4, 6, 8, 10, 12, 14, 16, 18, 20, 22, 24, 26, 32, 34, 36, 38, 40, 56, 68, and 80 as per kit instructions using the Quantikine ELISA Human CD14 Immunoassay kit (R&D Systems).

[8]MIG, monokine induced by gamma interferon
[9]VEGF, vascular endothelial growth factor
[10]HGF, hepatocyte growth factor
[11]EGF, epidermal growth factor
[12]FGF-Basic, fibroblast growth factor-basic
[13]MCP-1, monocyte chemoattractant protein-1
[14]IP-10, interferon gamma-induced protein 10
[15]IL-1RA, interleukin 1 receptor antagonist
[16]I-TAC, interferon-inducible T-cell alpha chemoattractant
[17]MDC, macrophage-derived chemokine
[18]MIF, macrophage migration inhibitory factor

Statistical Analyses

Data were prepared and analyzed using Prism 5 (Graphpad Software). Nonparametric tests were performed for MDSC frequency while parametric tests were utilized for cell suppression data. Paired analyses were utilized when appropriate. Nonparametric tests employed were Mann-Whitney U test for comparison of groups of unpaired data, Wilcoxon matched-pairs signed rank test for paired data and Spearman's rank-order correlation for X,Y correlation. Parametric tests employed were Student's unpaired T test for comparison of groups of unpaired data, Student's paired T test for comparison of groups of paired data and Pearson's correlation for X,Y correlation. An alpha of 0.0017 was used for cytokine correlations to adjust for multiple comparisons, otherwise an alpha of 0.05 was used for univariate analyses. Multiple regression analysis with stepwise selection was performed by SAS.

Results

MDSC frequency increases during SIV infection and after cART interruption

MDSC frequency was determined in two cohorts of rhesus macaques: a pilot study of 5 chronically SIV infected animals at 12 weeks post-infection (Fig. 1A) and a longitudinal study of 7 animals that were followed over the course of SIV infection and cART therapy starting 6 weeks after infection (Fig. 1B). A flow cytometry panel was optimized using blood from the pilot study to identify MDSC of granulocytic (gMDSC) or monocytic (mMDSC) origin in the Rhesus macaque model. MDSC frequencies were determined by the percent of singlet PBMC that were CD3−, HLA-DR−, CD11b+, and for gMDSC, CD66+, $SSC^{mid\text{-}high}$ while for mMDSC, CD66− and CD14+ (Fig. 1C).

We observed elevated frequencies of MDSC in the 5 chronically-SIV infected animals at 12 weeks post-infection compared to uninfected animals ($p=0.03$) (Fig. 2A). Total MDSC (Spearman $r=0.90$, $p=0.08$) and gMDSC (Spearman $r=1.00$, $p=0.02$) frequencies, but not mMDSC frequencies, trended or significantly correlated with viral load set-point, respectively (Fig. 2B).

We next embarked on a longitudinal study in a second set of 7 animals that were infected and cART initiated at 6 weeks post-infection. Here, we observed low MDSC frequency (median 0.18%) at pre-SIV infection time points in all 7 animals (Fig. 3A-C). MDSC frequency increased slightly, yet significantly, during acute infection at 2-3 weeks post-SIV challenge (median gain of 0.51%; $p<0.05$) in these animals (Fig. 3A-C). Combination antiretroviral therapy was initiated 6 weeks post-infection and MDSC frequency remained significantly elevated during cART (Fig. 3A-C). While MDSC levels during cART were stable in the majority of the animals (n=5), transient blips of elevated MDSC frequency were observed in two animals at weeks 14 & 36 for animal A14046 and at week 18 for animal A14047 (Fig 3D). Figure 3A-C shows summary data for clarity whereas Figure 3D shows the viral load kinetics vs. MDSC frequency at each time point for each animal individually. Animals A14041, A14043 and A14046 received a mock vaccination of empty plasmid vector while animals A14044, A14045, A14047 and A14048 received the empty plasmid vector plus a plasmid encoding the LT mucosal adjuvant. Although these control animals

received different plasmids, we observed no differences between MDSC frequencies in these control groups (data not shown).

At 37 weeks post-SIV infection (after 31 weeks on cART) drug therapy was withdrawn and MDSC were monitored to determine the effects of drug interruption on MDSC frequency and function. MDSC increased dramatically (median gain of 6.8%) over the first 20 weeks post-cART interruption (Fig. 3A-C). Although the drastic increase in frequency after stopping cART was transient, MDSC frequency remained elevated at 30 weeks post-cART interruption when compared to pre-SIV infection levels. Animals A14044 and A14047 were euthanized due to AIDS-defining illnesses before study completion (Fig. 3A-C †). Elevations in MDSC frequency after drug was stopped were comprised primarily by the granulocytic subset of MDSC (total MDSC were median 88% gMDSC) (Fig. 3B). Monocytic MDSC were infrequent in our study, only increasing significantly from baseline at 20 weeks post-cART interruption (Fig. 3C). This increase was much less marked (median gain of 0.26% from baseline) and also transient, returning to pre-SIV levels by week 68. We did not observe a correlation between MDSC frequency and CD4+ T cell or viral load levels (data not shown).

MDSC suppress SIV-specific and polyclonally stimulated T cell responses

To determine the effects of MDSC on T cell responses, we assayed the suppressive ability of MDSC for each animal 3 weeks pre-SIV infection, 3 weeks post-SIV infection, during cART (31 weeks after starting cART) and 19 weeks after stopping cART. We cultured PBMC in the presence or absence of MDSC with SEB (Fig. 4A) or SIV Gag peptide pool (Fig. 4B). T cell proliferation, measured by the expression of CD3 and Ki67, was suppressed in PBMC+MDSC wells compared to PBMC alone (Fig. 4AB). We found significant suppression by MDSC of SEB-stimulated responses at all time points (Fig. 4A). At time points where a sufficient response (>0.5%) to SIV Gag peptide pool was detected, we also observed significant suppression of SIV-specific T cell responses by MDSC (Fig. 4B). SIV-specific responses were more variable than SEB responses over the course of the study with low responses to SIV in most animals (Fig. 4C). Interestingly, the two animals with the highest and second-highest median SIV responses study-wide also had the lowest and third-lowest median MDSC frequency study-wide (Fig. 4C vs. 4D, animals A14043 and A14045, respectively).

As it appeared that MDSC had enhanced suppressive ability pre-SIV and on-cART SIV at weeks −3 and 31 (Fig. 4A), we compared suppressive ability between viremic (weeks 3 & 56) and aviremic (weeks −3 & 31) time points in each animal. MDSC suppression was not significantly different at viremic vs. uninfected or virally-suppressed time points (data not shown). MDSC suppressed both CD4+ and CD8+ T cell proliferation in response to SEB (Fig. 4E) and SIV peptide pool (Fig. 4F) at all time points. High density mature granulocytes can degranulate during cell death which may lead to non-specific suppression of T cell responses. In order to determine if viable gMDSC suppress T cell responses we performed a shorter T cell assay (18 hours instead of 4 days), using IFNγ release measured by ELISpot as a readout. gMDSC suppressed IFNγ release in response to SEB stimulus during an 18 hour co-incubation with MDSC-depleted PBMC in two independent experiments with

PBMC from 2 SIV+ rhesus macaques (data not shown). As 92% of MDSC were viable at 24 hours in culture (determined by a viability stain), we can conclude that viable gMDSC contribute to the majority of this suppression.

MDSC in lymphoid tissue exhibit suppressive function

Peripheral lymphoid organs were examined at necropsy to determine if MDSC infiltrate sites of T cell activation. We did not find elevated MDSC in lymph nodes when compared to MDSC levels in peripheral blood. However, there were elevated MDSC detected in the spleen that were comprised primarily of the granulocytic subset (Fig. 5A). Suppressive function of splenic gMDSC was determined in one animal. We found MDSC suppressed CD3+, CD4+ and CD8+ T cell proliferation in response to SEB to a level that was not observably different in the spleen vs. in the peripheral blood (Fig. 5B). We can, therefore, conclude that while no MDSC aggregation was apparent in peripheral lymph nodes at necropsy, MDSC function in peripheral blood is representative of other sites of MDSC accumulation.

Plasma cytokine levels correlate with MDSC

To determine if MDSC expansion was driven by inflammation during SIV infection, plasma cytokine levels were measured by ELISA and compared to frequency of MDSC measured at the same time points at study weeks −3, 3, 10, 14, 18, 37, 40, 46, 56, 68, and 80. There were direct and significant correlations, adjusted for multiple comparisons, between MDSC frequency and the magnitude of systemic inflammatory cytokines (Table I). IL-6 (Spearman $r=0.42$, $p=0.0003$), TNF (Spearman $r=0.48$, $p<0.0001$), MIP-1α (Spearman $r=0.47$, $p<0.0001$), MIF (Spearman $r=0.40$, $p=0.0005$), and IP-10 (Spearman $r=0.41$, $p=0.0004$) all correlated significantly with MDSC frequency (Table I and Fig. 6A). Correlations between many cytokines strengthened at time points where the animals were not on cART. During post-cART viremia (weeks 40-80), the correlation grew between MDSC frequency and TNF (Spearman $r=0.68$, $p<0.0001$), MIP-1α (Spearman $r=0.60$, $p=0.0003$), IL-6 (Spearman $r=0.58$, $p=0.0005$), IL-1β (Spearman $r=0.57$, $p=0.0007$), and MIP-1β (Spearman $r=0.54$, $p=0.0014$) (Fig. 6B).

HIV viral particles and HIV gp120 alone have been found to expand mMDSC in vitro (22). While plasma viral load trended towards correlating with MDSC frequency in our study, it did not reach statistical significance when adjusted for multiple analyses (Spearman $r= 0.44$, $p= 0.008$, data not shown). We also observed stronger correlations between MDSC and the inflammatory cytokines listed above, suggesting the inflammation induced by viremia rather than the viral particles themselves were having greater impact on MDSC frequency. Multivariate regression analysis with stepwise selection of the 29 cytokines assayed, including viral load data, showed that MIF and TNF independently correlated with MDSC frequency ($r^2=0.30$, $p<0.05$) throughout the study and TNF independently correlated in the post-cART viremic time points ($r^2=0.42$, $p<0.05$). This suggested MIF and TNF participate in MDSC accumulation or expansion in vivo. However, in vitro 2 day incubation of PBMC isolated from 2 additional animals during post-cART viremia at week 56 with 10ng/ml TNF did not result in gMDSC expansion in culture over media alone (data not shown).

Soluble CD14 levels increase during increased microbial translocation and predict HIV mortality (23). As the involvement of MIF and TNF indicated a potential contribution of microbial translocation to the generation of MDSC, we additionally assayed for sCD14 levels in plasma at study weeks 0, 2, 4, 6, 8, 10, 12, 14, 16, 18, 20, 22, 24, 26, 32, 34, 36, 38, 40, 56, 68, and 80. While viral loads were significantly lower post-cART interruption (week 40, 3 weeks post-cART interruption) compared to viral load in acute infection (week 4, 4 weeks post-SIV infection) (Fig. 6C), we observed a significant elevation in sCD14 at week 40 compared to week 4 (Fig. 6D). Examining sCD14 levels longitudinally there was not a marked increase of sCD14 immediately post-cART interruption but rather a slow increase over the weeks from SIV acute untreated to treated chronic SIV infection (Fig. 6E), indicating microbial translocation-mediated immune activation may be ongoing during cART.

Discussion

Previous studies have shown elevated MDSC in SIV and HIV infection compared to healthy controls, and a reduction of MDSC during cART-treatment. Our in-depth longitudinal analyses of MDSC kinetics in a rhesus macaque SIV infection model confirm that the frequency of total MDSC is indeed low pre-SIV infection as expected for otherwise healthy animals. Total MDSC frequency increased slightly but significantly during acute SIV infection, and this elevation was sustained even during effective cART. In the 20 weeks post-cART we observed a remarkable MDSC frequency increase for most animals, comprising 2-37% of total circulating PBMC. Of note, two of the three animals with the highest peak total MDSC frequencies were euthanized with AIDS-defining illnesses before the end-of-study, suggesting MDSC may have contributed to disease progression in these animals.

The granulocytic fraction of MDSC was the driver of the elevated MDSC observed. Thus, functional characterization focused on this subset. Using either the superantigen SEB or a SIV Gag peptide pool to stimulate T cell proliferation, we found that granulocytic MDSC were able to suppress SEB-stimulated T cell proliferation quite consistently at all study time points assayed and suppressed both CD4+ and CD8+ T cell proliferation in a dose-dependent manner. SIV peptide responses were more variable than the polyclonal SEB stimulus, but for all SIV proliferative responses over 0.5%, we observed suppression by MDSC. As the two animals with the highest SIV-specific T cell responses over the course of the study also had the lower median MDSC frequencies over the course of the study, this suggests MDSC may additionally be acting to inhibit activation or priming of naïve T cells.

In previous studies it has not been clear which subset, granulocytic or monocytic, is more relevant in HIV infection. Two groups reported elevation of mMDSC in HIV+ infected individuals with very low CD4 counts and at advanced clinical stage (18, 22). The majority of these HIV+ individuals in Qin et al.'s study (~70%) had very low CD4 counts (<200) with less than 10% of the population having a CD4 count above 350. The majority of patients (~70%) were also CDC classification C HIV clinical stage (experiencing AIDS-symptoms). Similarly, the HIV+ population studied by Garg et al. had a low median CD4 count of <200, and characterization of mMDSC expansion was observed when cultured and measured ex vivo. As for the studies where gMDSC were found to be elevated, the CD4 counts in HIV+

participants were higher with Vollbrecht et al. reporting an average CD4 count of 422 (range: 16-1237) (16) and Bowers et al. reporting a median CD4+ T cell count of 444 (range: 102–1,385) pre-cART and a median CD4+ T cell count of 657 (range: 189–1,763) on cART (17).

The granulocytic subset of MDSC comprised a median 90% of the total MDSC population over the course of SIV infection in our study. While the monocytic subset significantly increased at week 56 during the post-cART cytokine elevation, it still only comprised a median 5% of the total MDSC population at that time point. Our observations in combination with the previous published data suggest while granulocytic MDSC accumulate over time during chronic retroviral infection in otherwise healthy individuals, the monocytic subset may expand only during periods of poor health. As we also saw peak gMDSC frequencies at week 56 where the only significant increase in mMDSC was observed, this theory does not completely explain why Qin et al. did not find a functional and frequent granulocytic MDSC subset in their study. Cryopreservation of PBMC particularly reduces gMDSC frequency (24-26). The majority of the MDSC characterization by Qin et al. utilized cryopreserved specimens. Although in this study MDSC frequencies were compared in a subset of participants between cryopreserved and fresh PBMC, the primary use of cryopreserved specimens may have accounted for the difference in results whereas MDSC frequencies measured in our study were all determined using freshly isolated PBMC.

Others have reported MDSC infiltration of the spleen in the mouse tumor model (reviewed in (27)). We observed MDSC infiltration in the spleen of nonhuman primates but not in any other peripheral lymphoid organs at necropsy. Splenic MDSCs have been reported to be less suppressive than those at the tumor site (27), however we observed similar suppressive ability of splenic vs. peripheral blood MDSC. This suggests that while MDSC in the tumor microenvironment can acquire differential function, MDSC from the periphery and the spleen represent similar populations in SIV infection. In addition, while populations of MDSC were not found in lymph nodes at necropsy, the peak MDSC frequencies were achieved 24 weeks earlier for most animals. Whether MDSC traffic to lymph nodes and inhibit T cell activation or priming earlier in infection or immediately post cART-interruption remains an open question.

In previous studies MDSC correlated with CD4 count and viral load in HIV infection. We observed correlations with viral load in our pilot study and did not observe CD4 count correlation with MDSC in either study. In the pilot study, set-point viral loads were determined after 12 weeks of untreated infection and these did correlate with MDSC frequency at week 12. Animals were started on cART at week 6 post-infection in the longitudinal study. Viral loads correlate with MDSC frequencies in humans during untreated chronic infection (16-18). Therefore, the length of exposure to viremia may be a factor influencing cytokine elevation and MDSC generation and thus may explain the lack of a strong correlation in our longitudinal study where animals were treated at week 6 post-infection, and were aviremic for most of the treatment duration. The lack of correlation between CD4 counts and MDSC frequencies may be attributed to the relatively high CD4 count in our study (average 1150 CD4/ml study-wide) compared to the human studies

(reporting average CD4 counts below 500 for all studies) as the correlation between MDSC and CD4 may wane in healthy individuals or animals with very high CD4 counts (16-18).

Inflammatory cytokines and growth factors are known to induce MDSC expansion and enhance suppression in cancer (reviewed in (28)). Systemic levels of IL-6, TNF, MIP-1α, MIF, VEGF and IP-10 correlated with MDSC frequency over the course of the study and the peak cytokine levels were achieved 10-30 weeks post-cART interruption for most. IL-1β, IL-6, IP-10 and VEGF promote MDSC expansion and suppression by inducing myelopoiesis and activating transcription factors including STAT3, a master transcription factor for MDSC (1, 28, 29).

As HIV viral particles have been shown to induce mMDSC in vitro (22), we added viral load to our cytokine analyses. MDSC frequency strongly correlated with elevations in IL-6, IL-1β, TNF, MIP-1α and MIP-1β during the post-cART cytokine storm and these correlations were stronger than the correlation between viral load and MDSC frequency. This suggests to us that viral particles alone are not the sole contributors to MDSC expansion.

Linear regression with stepwise selection of the 29 cytokines in addition to viral load identified MIF and TNF as independently correlating with MDSC in our study. MIF is an inflammatory cytokine that is elevated in cancer and sepsis, and has been shown to enhance tumor progression by mMDSC induction (30). In HIV-infected individuals with evidence of microbial translocation, MIF levels have been found to be elevated compared to healthy controls (31), and MIF can be released in response to LPS (32) and during untreated HIV infection (33). MIF can also drive TNF production (32). TNF signaling appears integral to MDSC expansion in the mouse cancer model as TNF-receptor deficient mice exhibit decreased MDSC frequencies caused by decreased MDSC induction from the bone marrow and decreased survival (34). TNF can disrupt epithelial tight junctions and anti-TNF antibody treatment reduces this disruption (35). In addition, MDSC in a mouse cancer model secrete TNF (34), however the subset of MDSC responsible was not resolved. We hypothesized microbial translocation may have an impact on MIF and TNF elevation. We then observed that while levels of other circulating inflammatory cytokines were low during cART, sCD14, a marker for microbial translocation, progressively increased. We therefore hypothesize that contributions from microbial translocation despite cART therapy and from viral products post-cART treatment interruption, in combination, initiated and perpetuated the cytokine storm post-cART interruption driving MDSC production in our study.

Limitations of this work were the small specimen volume received at each time point. The number of cells available was only sufficient to define the population of MDSC by suppressive ability but not sufficient to perform mechanistic experiments. Additionally, as high density mature granulocytes can degranulate during cell death this may have led to non-specific suppression of T cell proliferative responses during the 4 day culture experiment. At 18 hours post-incubation, we detected MDSC-mediated suppression of IFNγ production indicating the suppression observed is not solely a bystander effect of MDSC degranulation due to cell death. Low-density neutrophils may have lower density due to either previous degranulation or the absence of mature granules (7, 8), therefore in 4 day culture the

contribution of granule contents on gMDSC induced T cell suppression may be much less than the contribution from mature neutrophils. We prioritized measurement of MDSC-mediated suppression of proliferative ability over IFNγ production because proliferative ability is the strongest independent predictor of HIV disease progression vs. disease control (12).

While post-necropsy cytokine analyses showed that TNF and MIF correlated with MDSC frequency, it is not clear if these cytokines directly expand MDSC in the rhesus macaque model. We examined the effect of TNF on MDSC frequency in 2-day ex vivo culture in two SIV+ rhesus macaques and did not observe an effect. The effect of TNF or MIF on expansion of gMDSC may not be measurable in vitro since there are no precursors to these cells in whole PBMC. We hypothesize these cytokines instead contribute to gMDSC accumulation by mobilizing granulocytic precursors from the bone marrow which then acquire suppressive function (34).

In lentiviral infection, poor clinical outcomes correlate both with systemic inflammation and poor proliferative ability of virus-specific T cells. We demonstrated that MDSC suppress SIV-specific T cell proliferative responses and found correlations between MDSC and several circulating inflammatory cytokines. In addition, we have identified a novel, transiently elevated population of gMDSC subsequent to cART treatment interruption. Plasma measurements suggest the possibility of a synergistic contribution of increasing microbial translocation despite cART and post-cART viral rebound that may be driving this population increase. Many of the curative HIV therapies under current investigation require a treatment interruption to determine efficacy of curative regimen. Our work suggests that these treatment interruptions may induce marked elevation of cells involved in immune regulation that may hamper the effectiveness of such strategies. Therapies to reduce MDSC frequency during SIV and HIV infection, especially post-cART treatment interruption, may enhance cellular immune responses and effectiveness of curative strategies.

References

1. Gabrilovich DI, Nagaraj S. Myeloid-derived suppressor cells as regulators of the immune system. Nature reviews. Immunology. 2009; 9:162–174.
2. Talmadge JE, Gabrilovich DI. History of myeloid-derived suppressor cells. Nature reviews. Cancer. 2013; 13:739–752.
3. Diaz-Montero CM, Salem ML, Nishimura MI, Garrett-Mayer E, Cole DJ, Montero AJ. Increased circulating myeloid-derived suppressor cells correlate with clinical cancer stage, metastatic tumor burden, and doxorubicin-cyclophosphamide chemotherapy. Cancer immunology, immunotherapy : CII. 2009; 58:49–59. [PubMed: 18446337]
4. Weed DT, Vella JL, Reis IM, De la Fuente AC, Gomez C, Sargi Z, Nazarian R, Califano J, Borrello I, Serafini P. Tadalafil reduces myeloid-derived suppressor cells and regulatory T cells and promotes tumor immunity in patients with head and neck squamous cell carcinoma. Clinical cancer research : an official journal of the American Association for Cancer Research. 2015; 21:39–48. [PubMed: 25320361]
5. Kusmartsev S, Cheng F, Yu B, Nefedova Y, Sotomayor E, Lush R, Gabrilovich D. All-trans-retinoic acid eliminates immature myeloid cells from tumor-bearing mice and improves the effect of vaccination. Cancer research. 2003; 63:4441–4449. [PubMed: 12907617]
6. Nagaraj S, Youn JI, Weber H, Iclozan C, Lu L, Cotter MJ, Meyer C, Becerra CR, Fishman M, Antonia S, Sporn MB, Liby KT, Rawal B, Lee JH, Gabrilovich DI. Anti-inflammatory triterpenoid

blocks immune suppressive function of MDSCs and improves immune response in cancer. Clinical cancer research : an official journal of the American Association for Cancer Research. 2010; 16:1812–1823. [PubMed: 20215551]

7. Mishalian I, Granot Z, Fridlender ZG. The diversity of circulating neutrophils in cancer. Immunobiology. 2016
8. Scapini P, Cassatella MA. Social networking of human neutrophils within the immune system. Blood. 2014; 124:710–719. [PubMed: 24923297]
9. Gervassi A, Lejarcegui N, Dross S, Jacobson A, Itaya G, Kidzeru E, Gantt S, Jaspan H, Horton H. Myeloid derived suppressor cells are present at high frequency in neonates and suppress in vitro T cell responses. PloS one. 2014; 9:e107816. [PubMed: 25248150]
10. Schmitz JE, Kuroda MJ, Santra S, Sasseville VG, Simon MA, Lifton MA, Racz P, Tenner-Racz K, Dalesandro M, Scallon BJ, Ghrayeb J, Forman MA, Montefiori DC, Rieber EP, Letvin NL, Reimann KA. Control of viremia in simian immunodeficiency virus infection by CD8+ lymphocytes. Science. 1999; 283:857–860. [PubMed: 9933172]
11. Elahi S, Dinges WL, Lejarcegui N, Laing KJ, Collier AC, Koelle DM, McElrath MJ, Horton H. Protective HIV-specific CD8+ T cells evade Treg cell suppression. Nature medicine. 2011; 17:989–995.
12. Ndhlovu ZM, Chibnik LB, Proudfoot J, Vine S, McMullen A, Cesa K, Porichis F, Jones RB, Alvino DM, Hart MG, Stampouloglou E, Piechocka-Trocha A, Kadie C, Pereyra F, Heckerman D, De Jager PL, Walker BD, Kaufmann DE. High-dimensional immunomonitoring models of HIV-1-specific CD8 T-cell responses accurately identify subjects achieving spontaneous viral control. Blood. 2013; 121:801–811. [PubMed: 23233659]
13. Brenchley JM, Price DA, Schacker TW, Asher TE, Silvestri G, Rao S, Kazzaz Z, Bornstein E, Lambotte O, Altmann D, Blazar BR, Rodriguez B, Teixeira-Johnson L, Landay A, Martin JN, Hecht FM, Picker LJ, Lederman MM, Deeks SG, Douek DC. Microbial translocation is a cause of systemic immune activation in chronic HIV infection. Nature medicine. 2006; 12:1365–1371.
14. Younas M, Psomas C, Reynes J, Corbeau P. Immune activation in the course of HIV-1 infection: Causes, phenotypes and persistence under therapy. HIV medicine. 2016; 17:89–105. [PubMed: 26452565]
15. Giorgi JV, Hultin LE, McKeating JA, Johnson TD, Owens B, Jacobson LP, Shih R, Lewis J, Wiley DJ, Phair JP, Wolinsky SM, Detels R. Shorter survival in advanced human immunodeficiency virus type 1 infection is more closely associated with T lymphocyte activation than with plasma virus burden or virus chemokine coreceptor usage. The Journal of infectious diseases. 1999; 179:859–870. [PubMed: 10068581]
16. Vollbrecht T, Stirner R, Tufman A, Roider J, Huber RM, Bogner JR, Lechner A, Bourquin C, Draenert R. Chronic progressive HIV-1 infection is associated with elevated levels of myeloid-derived suppressor cells. Aids. 2012; 26:F31–37. [PubMed: 22526518]
17. Bowers NL, Helton ES, Huijbregts RP, Goepfert PA, Heath SL, Hel Z. Immune suppression by neutrophils in HIV-1 infection: role of PD L1/PD-1 pathway. PLoS pathogens. 2014; 10:e1003993. [PubMed: 24626392]
18. Qin A, Cai W, Pan T, Wu K, Yang Q, Wang N, Liu Y, Yan D, Hu F, Guo P, Chen X, Chen L, Zhang H, Tang X, Zhou J. Expansion of monocytic myeloid-derived suppressor cells dampens T cell function in HIV-1-seropositive individuals. Journal of virology. 2013; 87:1477–1490. [PubMed: 23152536]
19. Gama L, Shirk EN, Russell JN, Carvalho KI, Li M, Queen SE, Kalil J, Zink MC, Clements JE, Kallas EG. Expansion of a subset of CD14highCD16negCCR2low/neg monocytes functionally similar to myeloid-derived suppressor cells during SIV and HIV infection. Journal of leukocyte biology. 2012; 91:803–816. [PubMed: 22368280]
20. Sui Y, Hogg A, Wang Y, Frey B, Yu H, Xia Z, Venzon D, McKinnon K, Smedley J, Gathuka M, Klinman D, Keele BF, Langermann S, Liu L, Franchini G, Berzofsky JA. Vaccine-induced myeloid cell population dampens protective immunity to SIV. The Journal of clinical investigation. 2014; 124:2538–2549. [PubMed: 24837435]
21. Fuller DH, Rajakumar PA, Wu MS, McMahon CW, Shipley T, Fuller JT, Bazmi A, Trichel AM, Allen TM, Mothe B, Haynes JR, Watkins DI, Murphey-Corb M. DNA immunization in

combination with effective antiretroviral drug therapy controls viral rebound and prevents simian AIDS after treatment is discontinued. Virology. 2006; 348:200–215. [PubMed: 16439000]

22. Garg A, Spector SA. HIV type 1 gp120-induced expansion of myeloid derived suppressor cells is dependent on interleukin 6 and suppresses immunity. The Journal of infectious diseases. 2014; 209:441–451. [PubMed: 23999600]
23. Sandler NG, Wand H, Roque A, Law M, Nason MC, Nixon DE, Pedersen C, Ruxrungtham K, Lewin SR, Emery S, Neaton JD, Brenchley JM, Deeks SG, Sereti I, Douek DC, Group ISS. Plasma levels of soluble CD14 independently predict mortality in HIV infection. The Journal of infectious diseases. 2011; 203:780–790. [PubMed: 21252259]
24. Grutzner E, Stirner R, Arenz L, Athanasoulia AP, Schrodl K, Berking C, Bogner JR, Draenert R. Kinetics of human myeloid-derived suppressor cells after blood draw. Journal of translational medicine. 2016; 14:2. [PubMed: 26733325]
25. Kotsakis A, Harasymczuk M, Schilling B, Georgoulias V, Argiris A, Whiteside TL. Myeloid-derived suppressor cell measurements in fresh and cryopreserved blood samples. J Immunol Methods. 2012; 381:14–22. [PubMed: 22522114]
26. Trellakis S, Bruderek K, Hutte J, Elian M, Hoffmann TK, Lang S, Brandau S. Granulocytic myeloid-derived suppressor cells are cryosensitive and their frequency does not correlate with serum concentrations of colony-stimulating factors in head and neck cancer. Innate immunity. 2013; 19:328–336. [PubMed: 23160385]
27. Kumar V, Patel S, Tcyganov E, Gabrilovich DI. The Nature of Myeloid-Derived Suppressor Cells in the Tumor Microenvironment. Trends in immunology. 2016
28. Gabrilovich DI, Ostrand-Rosenberg S, Bronte V. Coordinated regulation of myeloid cells by tumours. Nature reviews. Immunology. 2012; 12:253–268.
29. Wu L, Du H, Li Y, Qu P, Yan C. Signal transducer and activator of transcription 3 (Stat3C) promotes myeloid-derived suppressor cell expansion and immune suppression during lung tumorigenesis. Am J Pathol. 2011; 179:2131–2141. [PubMed: 21864492]
30. Simpson KD, Templeton DJ, Cross JV. Macrophage migration inhibitory factor promotes tumor growth and metastasis by inducing myeloid-derived suppressor cells in the tumor microenvironment. Journal of immunology. 2012; 189:5533–5540.
31. Santos-Oliveira JR, Regis EG, Giacoia-Gripp CB, Valverde JG, Alexandrino-de-Oliveira P, Lindoso JA, Goto H, Oliveira-Neto MP, Guerra JO, Grinsztejn B, Jeronimo SB, Morgado MG, Da-Cruz AM. Microbial translocation induces an intense proinflammatory response in patients with visceral leishmaniasis and HIV type 1 coinfection. The Journal of infectious diseases. 2013; 208:57–66. [PubMed: 23539743]
32. Calandra T, Roger T. Macrophage migration inhibitory factor: a regulator of innate immunity. Nature reviews. Immunology. 2003; 3:791–800.
33. Delaloye J, De Bruin IJ, Darling KE, Reymond MK, Sweep FC, Roger T, Calandra T, Cavassini M. Increased macrophage migration inhibitory factor (MIF) plasma levels in acute HIV-1 infection. Cytokine. 2012; 60:338–340. [PubMed: 22898393]
34. Zhao X, Rong L, Zhao X, Li X, Liu X, Deng J, Wu H, Xu X, Erben U, Wu P, Syrbe U, Sieper J, Qin Z. TNF signaling drives myeloid-derived suppressor cell accumulation. The Journal of clinical investigation. 2012; 122:4094–4104. [PubMed: 23064360]
35. Nazli A, Chan O, Dobson-Belaire WN, Ouellet M, Tremblay MJ, Gray-Owen SD, Arsenault AL, Kaushic C. Exposure to HIV-1 directly impairs mucosal epithelial barrier integrity allowing microbial translocation. PLoS pathogens. 2010; 6:e1000852. [PubMed: 20386714]

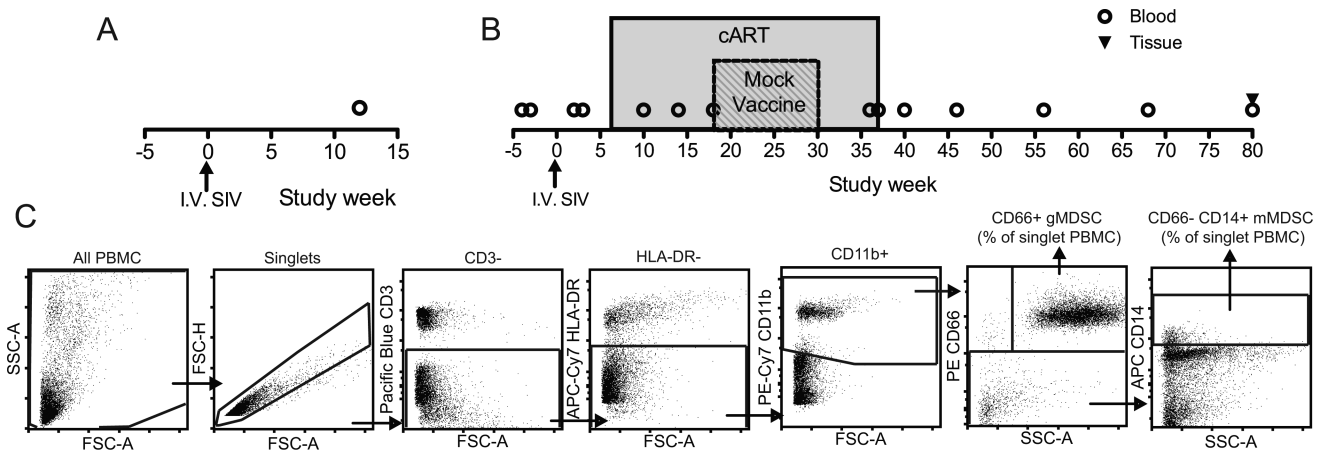

FIGURE 1.

Study design and gating strategy. **(A)** Design of pilot study. MDSC frequency of total peripheral blood PBMC was measured in freshly isolated PBMC at 12 weeks SIV post-infection (n=5) and compared to PBMC from uninfected animals (n=8). **(B)** Design of longitudinal study. MDSC frequency was measured in freshly isolated peripheral blood PBMC at study weeks −4, −3, 2, 3, 10, 14, 18, 36, 37, 40, 46, 56, 68 and in both tissue and blood at week 80. Animals were infected with SIV at study week 0, followed for 6 weeks of untreated infection then placed on cART for 31 weeks. During cART a mock vaccination of empty vector plasmid or empty vector plasmid plus plasmid-encoded heat labile *E. coli* enterotoxin (LT) mucosal adjuvant was delivered by gene gun at weeks 18, 22, 26 and 30. At week 37 the animals were taken off cART and followed to week 80. **(C)** Gating strategy for gMDSC was all PBMC, singlets, CD3−, HLA-DR−, CD11b+, and for gMDSC, CD66+, $SSC^{mid\text{-}high}$ while for mMDSC, CD66− and CD14+. Frequency of gMDSC and mMDSC was determined from all singlet PBMC.

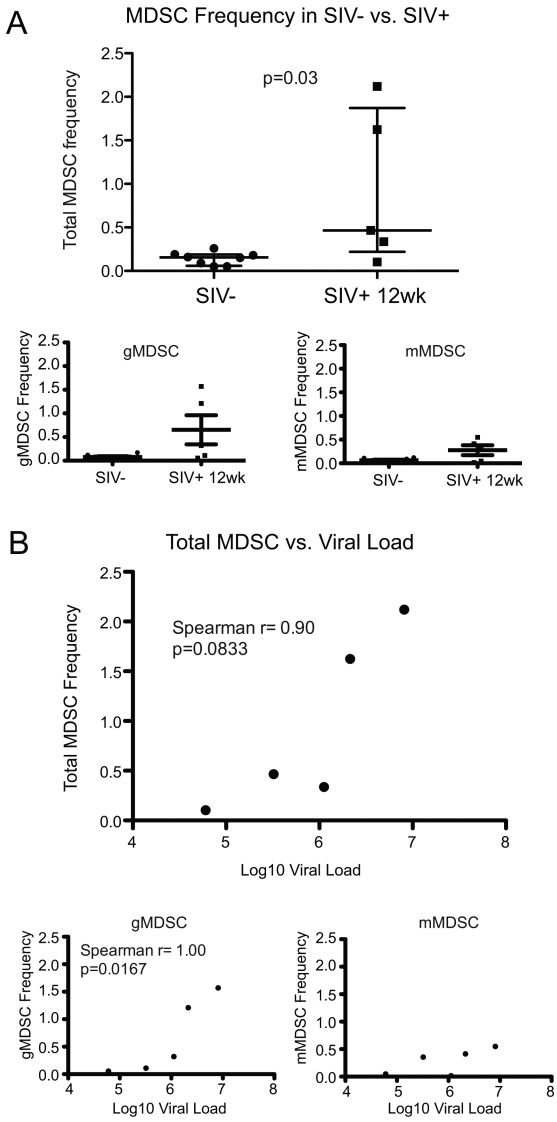

FIGURE 2.

MDSC frequency is elevated in chronic untreated SIV infection and correlates with set-point viral load. **(A)** Monocytic MDSC (mMDSC), granulocytic MDSC (gMDSC) and total MDSC frequencies were compared between SIV-uninfected animals (n=8) and SIV-infected animals (n=5) 12 weeks post-SIV infection. Significantly elevated MDSC frequencies were observed 12 weeks post-SIV infection in total MDSC frequency (of singlet PBMC). **(B)** Correlation analysis of frequencies of total MDSC, gMDSC and mMDSC with set-point viral loads in 5 SIV infected animals. Significant ($p<0.05$) and trending ($p<0.10$) correlation were determined by Mann-Whitney U test **(A)** and Spearman's rank correlation coefficient **(B).**

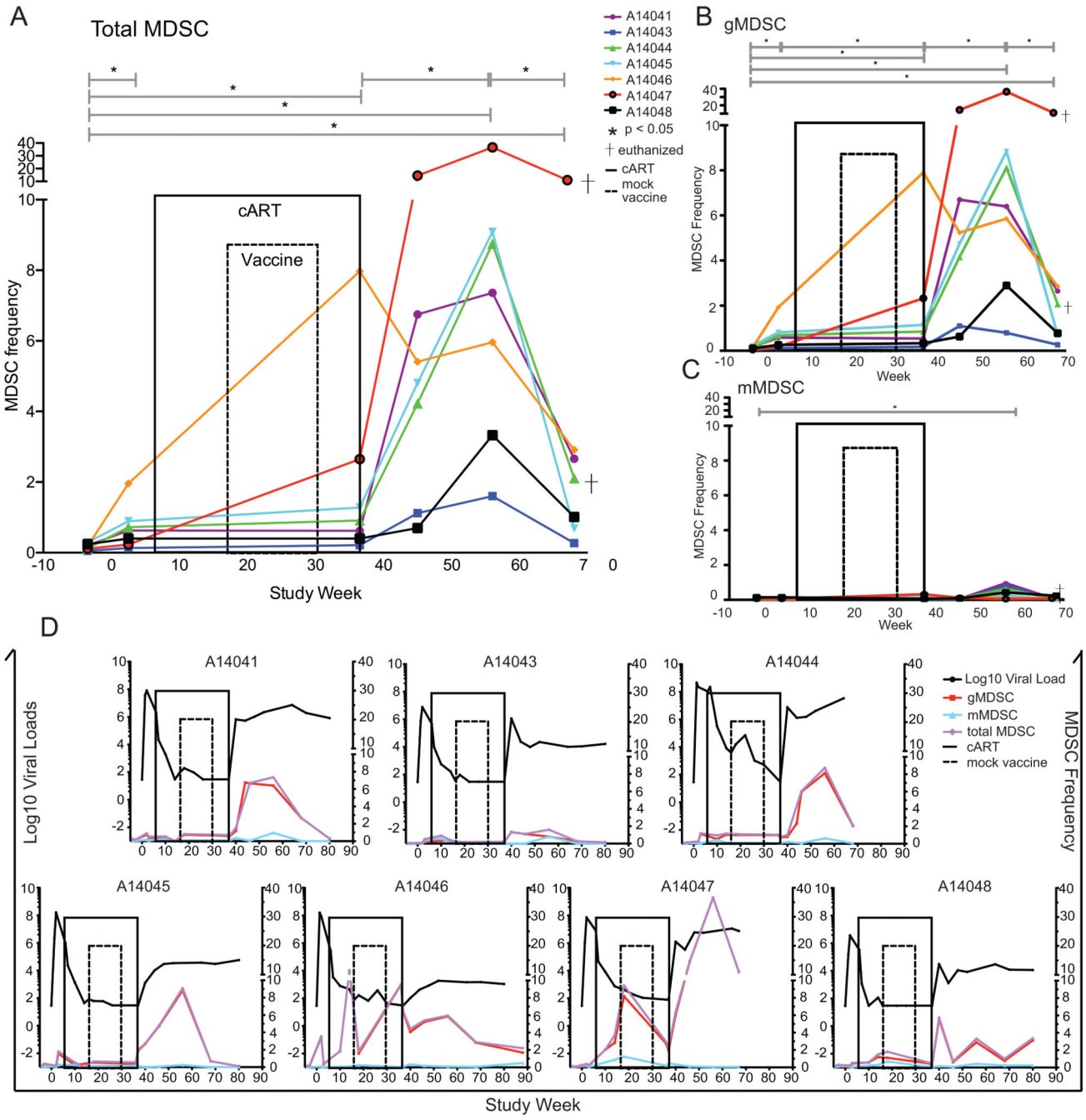

FIGURE 3.

Longitudinal MDSC frequency kinetics in 7 animals over the course of SIV infection, cART treatment, mock vaccination and cART-interruption. **(A-C)** Total MDSC (**A**), gMDSC (**B**) and mMDSC (**C**) frequency kinetics over time. Animals were SIV-infected on week 0 IV with SIV/DeltaB670. On week 6 animals were treated with cART consisting of daily subcutaneous Viread (PMPA, 20 mg/kg) and Emtriva (FTC, 30 mg/kg until viral suppression then 20 mg/kg), and twice-daily oral Isentress (Raltegravir, 200mg/kg first 30 days treatment then 165mg/kg) until week 37. At study weeks 18, 22, 26 and 30 animals were vaccinated with mock vaccine consisting of an empty plasmid vector +/− plasmid-encoded LT mucosal

adjuvant. Animals A14041 (purple), A14043 (blue) and A14046 (orange) received a mock vaccination of empty plasmid vector while animals A14044 (green), A14045 (light blue), A14047 (red) and A14048 (black) received empty plasmid vector plus mucosal adjuvant. Animals A14044 and A14047 were euthanized due to AIDS-defining illnesses before study completion (†). Two replicate MDSC frequencies were averaged at weeks −4 and −3 pre-SIV infection, weeks 2 and 3 post-SIV infection and weeks 36 and 37 pre-cART treatment interruption then independent measures of MDSC frequencies were graphed at study weeks 46, 56 and 68. **(D)** Log10 SIV viral loads were charted with individual MDSC measurements for each animal. MDSC frequencies were compared by Wilcoxon matched-pairs signed rank test. Vaccination group MDSC frequencies were compared by Mann-Whitney U test.

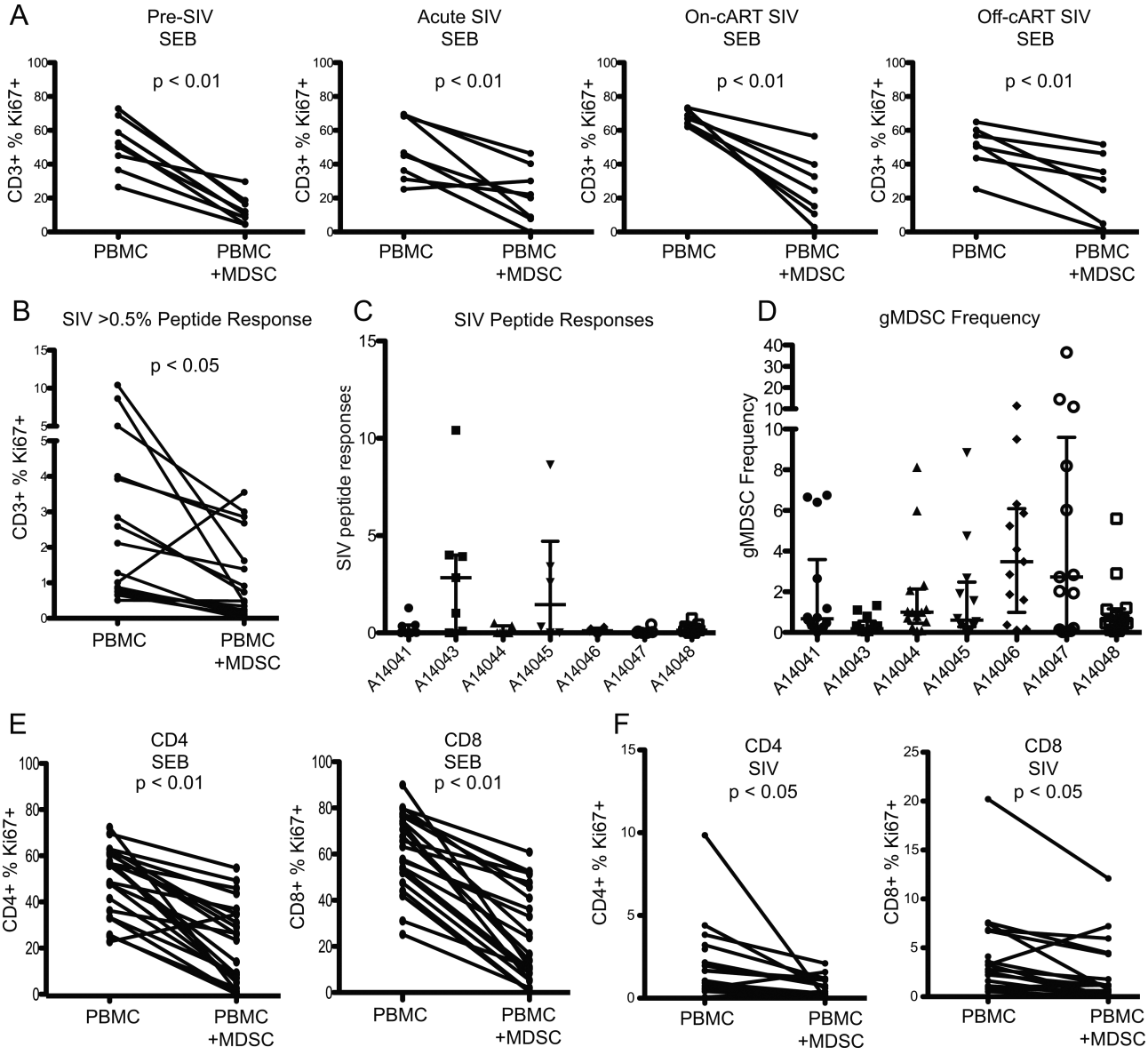

FIGURE 4.

gMDSC suppress T cell responses to SEB and SIV Gag peptide stimuli. CD66+ gMDSC were depleted from PBMC and cultured either alone or with CD66+ MDSC at a 1:1 ratio overnight, then stimulated with 0.4ug/ml superantigen Staphylococcal enterotoxin B (SEB) from *Staphylococcus aureus* **(A)** or 1ug/ml 15mer SIVmac239 gag peptide pool (**B-C**) for 4 days. Proliferation of CD3+ cells was measured by ICS for Ki67. **(D)** median gMDSC frequency study-wide. **(E-F)** CD66+ MDSC suppression of CD4+ and CD8+ T cells when stimulated with SEB (E) and SIV Gag peptide pool (F). Percent of Ki67+ CD3+, CD4+ and CD8+ cells were compared by Wilcoxon matched-pairs signed rank test.

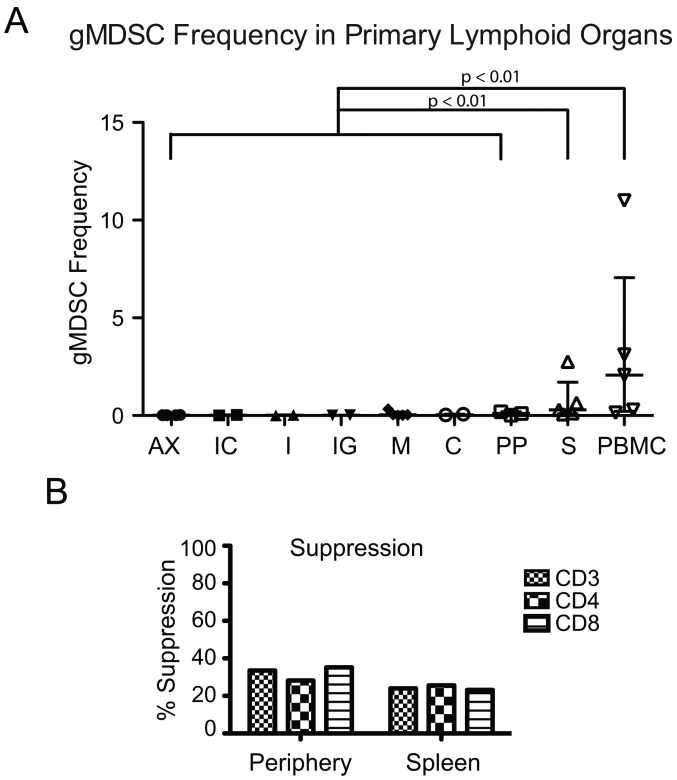

FIGURE 5.

gMDSC frequency in peripheral lymphoid organs. **(A)** Peripheral lymphoid organs were excised at necropsy and examined for MDSC infiltration. Single-cell suspensions of axillary (AX), ileocecal (IC), iliac (I), inguinal (IG), mesenteric (M), cervical/ retropharyngeal (C) lymph nodes as well as ileum (PP) and spleen (S) were density separated by Ficoll gradient centrifugation and stained for MDSC. **(B)** Suppression of T cell proliferation in response to SEB of CD66− PBMC by co-culture with MDSC at a 1:1 ratio. Suppression of T cell proliferation was compared in PBMC isolated from the spleen or the peripheral blood. MDSC frequencies in lymph node vs. spleen and ileum were compared by Kruskal-Wallis one-way analysis of variance. ** $p<0.01$

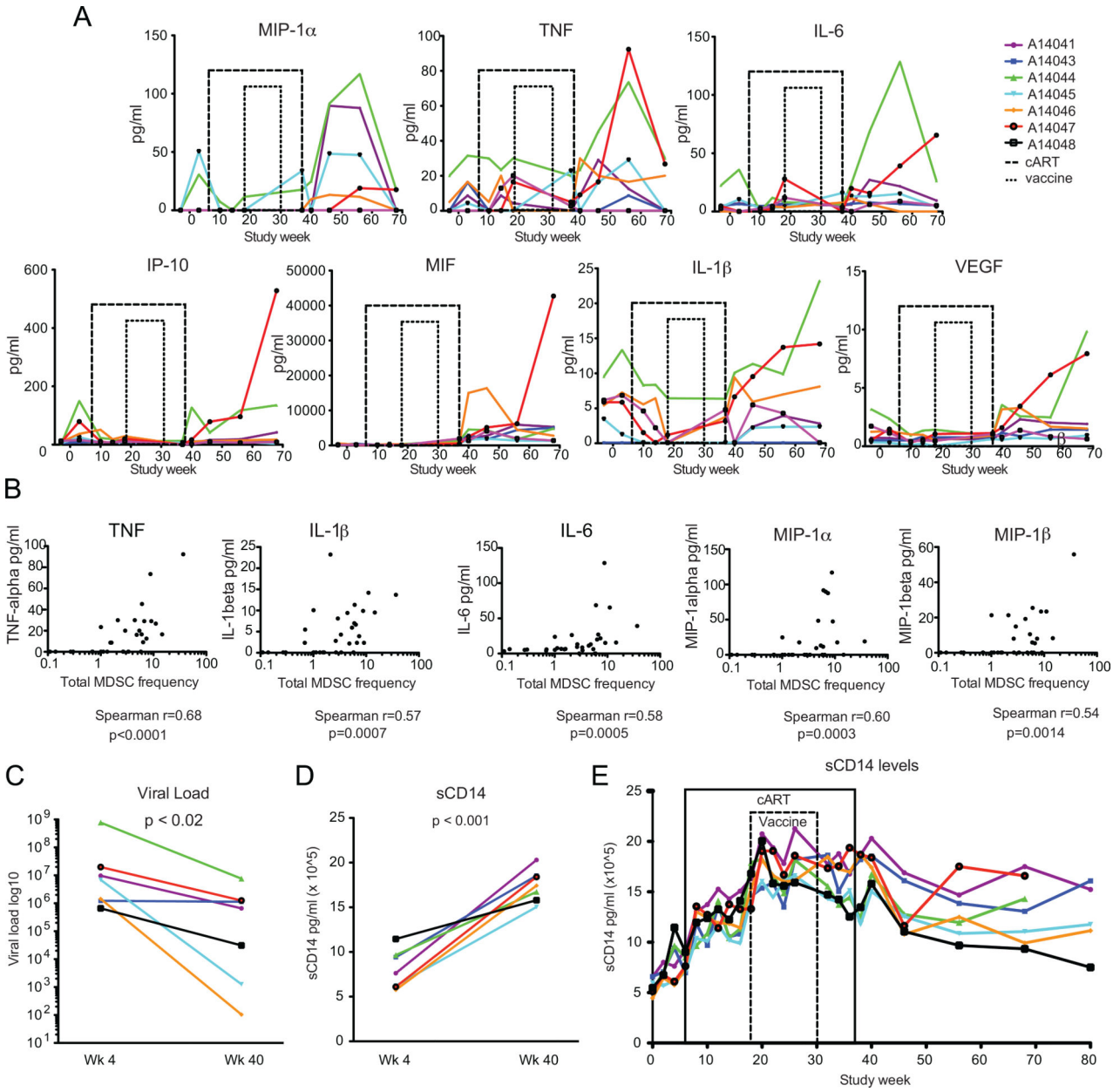

FIGURE 6.

Longitudinal analysis of plasma inflammatory cytokine kinetics. Plasma was batch tested for the following cytokines, chemokines and growth factors: GMCSF, TNF, IL-1β, IL-4, IL-6, MIG, VEGF, HGF, EGF, IL-8, IL-17, MIP-1α, IL-12, IL-10, FGF-Basic, IFN-γ, G-CSF, MCP-1, IL-15, IP-10, MIP-1β, Eotaxin, RANTES, IL-1RA, I-TAC, MDC, IL-5, IL-2 and MIF at weeks -3, 3, 10, 14, 18, 37, 40, 46, 56 and 68. sCD14 levels were assessed at weeks 0, 2, 4, 6, 8, 10, 12, 14, 16, 18, 20, 22, 24, 26, 32, 34, 36, 38, 40, 56, 68, and 80. **(A)** Cytokine kinetics are shown for MIP-1α&β, TNF, IL-6, IP-10, MIF, IL-1β, and VEGF. **(B)** Correlation analyses are shown between MDSC and TNF, MIP-1α&β, IL-6, IL-1β during post-cART viremia. **(C)** Viral load comparison between 4 weeks post-infection (wk 4) and 3 weeks post-cART interruption (wk 40), (**D**) sCD14 comparison between 4 weeks post-

infection (wk 4) and 3 weeks post-cART interruption (wk 40). **(E)** Longitudinal analysis of sCD14 levels over time. Cytokines were correlated by Spearman's rank correlation coefficient. Viral loads and sCD14 levels were compared by paired t test.

TABLE I

MDSC frequencies correlate with circulating inflammatory cytokines[1]

Cytokine/chemokine/growth factor vs. MDSC frequency	Spearmanr	95% confidence interval	P value (two-tailed)	Is the correlation significant? (alpha=0.0017)
MIP-1α	0.4739	0.2673 to 0.6389	< 0.0001	Yes
TNF	0.4834	0.2786 to 0.6461	< 0.0001	Yes
IL-6	0.4158	0.1987 to 0.5940	0.0003	Yes
IP-10	0.4061	0.1874 to 0.5864	0.0004	Yes
MIF	0.3975	0.1776 to 0.5797	0.0005	Yes
IL-1β	0.3480	0.1214 to 0.5402	0.0026	no
VEGF	0.3255	0.09627 to 0.5220	0.005	no
IL-2	0.3164	0.08616 to 0.5145	0.0064	no
IL-4	−0.3065	−0.5065 to −0.07534	0.0083	no
MIP-1β	0.2905	0.05776 to 0.4932	0.0127	no
I-TAC	0.2843	0.05111 to 0.4882	0.0148	no
IL-10	0.2674	0.03279 to 0.4741	0.0222	no
EGF	0.2599	0.02475 to 0.4678	0.0264	no
IL-8	0.2505	0.01471 to 0.4599	0.0325	no
MCP-1	0.2504	0.01458 to 0.4598	0.0326	no
IL-1RA	0.2114	−0.02665 to 0.4267	0.0727	no
EOTAXIN	0.2112	−0.02679 to 0.4266	0.0728	no
IL-17	−0.1841	−0.4032 to 0.05500	0.119	no
FGF-Basic	0.1831	−0.05604 to 0.4023	0.1211	no
GM-CSF	−0.1694	−0.3904 to 0.07008	0.1519	no
MDC	0.145	−0.09492 to 0.3690	0.2209	no
IL-5	−0.1274	−0.3534 to 0.1127	0.2829	no
IL-15	−0.103	−0.3316 to 0.1371	0.3861	no
G-CSF	0.08559	−0.1542 to 0.3159	0.4715	no
HGF	0.07521	−0.1644 to 0.3064	0.5271	no
RANTES	−0.07173	−0.3033 to 0.1678	0.5465	no
MIG	0.05932	−0.1799 to 0.2919	0.6181	no
IFNγ	0.04994	−0.1890 to 0.2833	0.6748	no
IL-12	0.04723	−0.1916 to 0.2808	0.6915	no

[1] Plasma was batch-tested as per kit instructions using the Monkey Cytokine Magnetic 29-Plex Panel (ThermoFisher) for each cytokine, chemokine or growth factor listed. Cytokine levels were correlated to MDSC frequency by Spearman's rank correlation coefficient with an adjusted alpha of 0.0017 to account for multiple comparisons.